Arabian Journal of Chemistry (2023) **16**, 105175

King Saud University

Arabian Journal of Chemistry

www.ksu.edu.sa
www.sciencedirect.com

ORIGINAL ARTICLE

Pharmacokinetic investigation on the mechanism of interaction of anti-breast cancer calycosin with albumin: *In vitro*

Xuan Fang [a,b,c,d,e], **Jun Li** [f], **Min Zhang** [a,b,c,d,e], **Lu Yang** [a,b,c,d,e], **Yuyun Wang** [a,b,c,d,e], **Xu Liu** [a,b,c,d,e], **Jin Zhang** [a,b,c,d,e,*]

[a] *The 3rd Department of Breast Cancer, China Tianjin Breast Cancer Prevention, Treatment and Research Center, Tianjin Medical University Cancer Institute and Hospital, Tianjin, China*
[b] *Key Laboratory of Breast Cancer Prevention and Therapy of Ministry of Education; Tianjin, China*
[c] *Key Laboratory of Cancer Prevention and Therapy, Tianjin, China*
[d] *Tianjin's Clinical Research Center for Cancer, Tianjin, China*
[e] *Tianjin Medical University, Ministry of Education, National Clinical Research Center for Cancer, Tianjin, China*
[f] *Shanghai Tenth People's Hospital, Shanghai, China*

Received 30 May 2023; accepted 14 July 2023
Available online 20 July 2023

KEYWORDS

Human serum albumin;
Calycosin;
Interaction;
Breast cancer cell

Abstract It has been documented that calycosin induces anticancer effects against a wide range of cancer cells, *in vitro*. However, pharmacokinetic characteristics of calycosin based on its interaction with albumin as a main carrier protein as well as corresponding anticancer mechanisms remain largely unknown. Herein, we inquired into the interaction of calycosin with human serum albumin (HSA) by a wide range collection of spectroscopic and theoretical data. Also, anticancer effects of calycosin on breast cancer cells, MDA-MB 231, were explored by cell viability, lactate dehydrogenase (LDH), caspase-3 activity, and real-time PCR assays. The findings demonstrated that the quenching process resulting from the interaction of calycosin and HSA was largely static in nature and that the calycosin-HSA system spontaneously forms. Cellular and molecular studies revealed that calycosin did not induce a significant cytotoxic effect on the viability of normal human breast epithelial cells, (MCF-10A), even at 200 μM concentration at which it was able to inhibit the proliferation of breast cancer MDA-MB 231 cells up to 50%. Then, it was disclosed that calycosin can disrupt the membrane integrity and induces apoptosis in MDA-MB 231 cells through overexpression of caspase-3 mRNA, down regulation of Bcl-2, and elevation of caspase-3 mRNA and activity mediated by downregulation of mTOR and Akt mRNA. Therefore, it was realized that in breast cancer MDA-MB 231 cells, calycosin is able to suppress cellular proliferation via apoptosis, which is controlled by the Akt/mTOR signaling cascade.

* Corresponding authors at: Tianjin Medical University Cancer Institute and Hospital, Huanhuxi Road, He Xi District, Tianjin 300060, China.
E-mail address: zhangjintjmuch1@163.com (J. Zhang).

https://doi.org/10.1016/j.arabjc.2023.105175
1878-5352 © 2023 The Authors. Published by Elsevier B.V. on behalf of King Saud University.

1. Introduction

Calycosin, 7-hydroxy-3-(3-hydroxy-4-methoxyphenyl)chromen-4-one, is a hydroxyisoflavone substance extracted widely from the dry root extract *Radix astragali* (Gao et al., 2014). It has received extensive attention for the last decade because of its broad range of potential pharmaceutical and biomedical characteristics, including anti-inflammatory (Dong et al., 2018), anti-oxidant (Wang et al., 2023), anti-viral (Chen et al., 2011), anti-bacterial (Liu et al., 2020), anti-diabetics (Huang et al., 2022), and anti-cancer (Qu et al., 2022, Song et al., 2023, Wei et al., 2023) features. Furthermore, calycosin has been shown to induce the potential of inhibiting the proliferation of cancer cells through different pathways, including HOTAIR/p-Akt (Chen et al., 2015a), IGF-1R and p38 MAPK (Chen et al., 2014a), ERβ/miR-17 (Chen et al., 2015b), and WDR7-7-GPR30 (Tian et al., 2017). Calycosin seems to be a safe, non-toxic, and attractive alternative for a number of new drugs. But, the interaction of the calycosin with carrier proteins should be studied in advance to explore their pharmacodynamics properties. In fact, the bioavailability, biostability, absorption, and clinical use of small molecules can be regulated after its interaction with human serum proteins (Takahashi et al., 1980). In other words, binding of calycosin to human serum albumin (HAS) can be examined to provide insight to its future *in vivo* pharmacokinetics.

HSA with a mainly α-helical structure is known as one of the main carrier proteins in the blood which binds to a large number of ligands, including fatty acids, and small molecules (Kragh-Hansen, 1990). It has also served as a major carrier protein for several pharmacotherapeutic agents (Liu et al., 2015). It has been widely documented that several isoflavones, including genistein (Roy et al., 2013), soybean isoflavones (Zhao and Ren, 2009), biochanin A (Xue et al., 2017), and puerarin (He et al., 2008) can interact with HSA with high binding affinity and induce some conformational changes of protein, associated with the several parameters including structure of small molecules, hydroxylation, glycosylation, and presence of ions.

On the other hand, as breast cancer has been spreading widely in the recent years and different therapeutic modalities have not triggered significant anticancer effects, we aimed to explore the anticancer mechanism of calycosin against triple negative breast cancer, MDA-MB-231. As a matter of fact, the persistent upregulation of the mammalian target of rapamycin (mTOR)/Akt proliferation signaling pathway in tumor cells has elicited consequential interest in inhibiting this mechanism to combat the survival of cancer cells (Memmott and Dennis, 2009). It has been suggested that the Akt signaling pathway may play a key role in tumorigenesis, acting as a pro-oncogenic mediator by inhibiting apoptosis (Memmott and Dennis, 2009). Therefore, we assessed whether calycosin is able to trigger apoptosis in MDA-MB-231 cancer cells via inhibiting AKT/mTOR pathway and regulating Bcl-2, Bax, and caspase-3 mRNA as main modulators of apoptosis.

2. Materials and methods

2.1. Materials

Human serum albumin (HSA), calycosin, RPMI-1640, 3-(4,5-dimethylthialzol-a-yl)-2,5-diphenyltetrazolium bromide (MTT), and fetal bovine serum (FBS), were purchased from Sigma-Aldrich (St. Louis, MO, USA). Human breast cancer cell MDA-MB-231 and normal human breast epithelial cell MCF-10A were obtained from the American Type Culture Collection (Manassas, VA, USA). The HSA concentration was determined spectrophotometrically with an extinction coefficient of 35,700 $M^{-1}cm^{-1}$ at 280 nm using UV–vis spectrophotometer (Perkin Elmer model).

2.2. Intrinsic fluorescence spectroscopy

Fluorescence spectroscopy analyses were done on a Hitachi fluorescence spectrophotometer (MPF-4) having a thermostat bath as well as a 1.0 cm quartz cell. The HSA sample (2 μM) was titrated with increasing concentrations of calycosin (0–80 μM). *Ex* wavelength was set at 280 nm and the *Em* wavelength was recorded in the range of 290 to 440 nm, while both band widths were set at 5 nm at three temperatures of 298, 308 and 318 K.

To determine the quenching mechanism, the well-known Stern–Volmer Eq. (1) was used as follows (Zhao et al., 2022):

$$F_0/F = 1 + k_q\tau_0[calycosin] = 1 + K_{SV}[calycosin] \quad (1)$$

where F_0 and F are the fluorescence intensities without and with ligand (calycosin), respectively, k_q is the protein quenching constant, τ_0 is the life time of the protein without ligand, which is around 10^{-8} s, and K_{SV} is the Stern–Volmer quenching constant (Zhao et al., 2022).

The K_{SV} value can be estimated using the slope of the linear plot of F_0/F against [calycosin]. Furthermore, a modified Stern–Volmer Eq. (2) was utilized for the calculation of binding constant (K_b) and the number of binding sites (n) as follows:

$$\log(\Delta F)/F = \log K_b + n\log[calycosin] \quad (2)$$

The binding parameters can be then calculated from the slope of log $(\Delta F)/F$ versus log [calycosin].

To determine the binding forces, the van't Hoff Eq. (3) and Gibbs-Helmholtz Eq. (4) were used as follows (Zargar et al., 2022):

$$\ln K_b = -\Delta H^{\circ}/RT + \Delta S^{\circ}/R \quad (3)$$

$$\Delta G^{\circ} = \Delta H^{\circ} - T\Delta S^{\circ} \quad (4)$$

Standard enthalpy changes ($\Delta H°$), Standard entropy changes ($\Delta S°$), and Standard Gibbs free energy changes ($\Delta G°$) were than calculated by these Eqs. The value of K_b as a binding constant can be plotted versus corresponding temperature (T) to calculate $\Delta H°$ and $\Delta S°$ values from the slope and the Y-intercept, respectively. R is the gas constant (8.314 J/mol K).

2.3. Circular dichroism spectroscopy

Circular dichroism (CD) study was done using an Aviv model 215 spectropolarimeter (Lakewood, NJ, USA) equipped with a 1.0 mm path length cell. The far-UV CD spectra of HSA (5 μM) were read after incubation with increasing concentrations of calycosin (0, 10, 80 μM) in the range of 200–250 nm with a bandwidth 1 nm, and at a temperature of 298 K under constant nitrogen gas. The amounts of secondary structures of HSA were determined by using CDNN software.

2.4. Molecular docking

The molecular docking study was carried out with the AutoDock Vina program. The crystal structure of HSA with PDB ID: 1AO6 was obtained from the Protein Data Bank (https://www.rcsb.org/structure/1ao6). Also, the three-dimensional structure of calycosin with PubChem ID:

5280448 was downloaded from PubChem (https://pubchem.ncbi.nlm.nih.gov/compound/calycosin). The molecular docking runs were done on the Autodocking engine with blind candidate sites and calycosin was selected as a flexible ligand. The free binding energy was calculated based on 10 different poses.

2.5. Cell culture and MTT assay

The breast cancer cell MDA-MB-231 and normal human breast epithelial cell MCF-10A were cultured in RPMI-1640 medium supplemented with 10% FBS, and 1% streptomycin/penicillin. These cells were incubated at 37 °C in a humidified incubator with 5% CO_2. After reaching the proper density, the cells were used for further assays. Cell viability was assessed after treatment of the cells by different concentrations of calycosin (1–200 μM) for 48 by using MTT assay as previously described (Fattahian Kalhor et al., 2020).

2.6. LDH assay

The activity of lactate dehydrogenase (LDH) in cell culture medium was assessed according to the manufacturer's protocols (LDH assay kit, TOX7, Sigma, USA). Briefly, cells were incubated with IC50 concentrations of calycosin for 48 h, then 100 μL/well of supernatant was added by 100 μL of LDH reaction mixture, and incubated for 3 h incubation. Finally, the absorbance of the samples was read at 490 nm using a Microplate Reader.

2.7. Caspase 3,7 activity

Caspase 3,7 activity assay was done based on the protocols provided by Caspase-3 Assay Kit (Colorimetric) (ab39401). Briefly, after treatment with 200 μM calycosin for 48 h, the cells were washed with cold PBS, collected, centrifuged (2000 rpm, 10 min), resuspended, lysed at 4 °C for 30 min, and centrifuged (10000 rpm, 20 min). After collection of supernatants, a fixed concentration of samples was mixed with a working solution and incubated for 2 h at 37 °C. Finally, the absorbance of each sample was detected at 405 nm using an ELISA plate reader (RT-2100C Microplate Reader, China).

2.8. Real-time PCR

A number of 1×10^5 MDA-MB-231 cells were seeded and incubated with 200 μM calycosin for 48 h at 37 °C and 5% CO_2. The harvested cells were washed, centrifuged (1000 rpm, 5 min) and used for RNA extraction using RNA Extraction Kit (Thermo Fisher Scientific, USA) following its protocol, and its quality was determined by using a nanodrop spectrophotometer (Thermo Scientific Scientific, USA). Synthesis of cDNA was then carried out using RevertAid First Strand cDNA Synthesis Kit (Thermo Fisher Scientific, USA) following its protocol. The expression of genes at RNA level in MDA-MB-231 cells after incubation with calycosin was measured semi-quantitatively in comparison with control group (untreated MDA-MB-231 cells) using qRT-PCR technique, based on the previous study (Liu et al., 2018). The relative gene expression was determined using a $2^{-\Delta Ct}$ method (Schmittgen and Livak, 2008), and data was normalized relative to GAPDH.

2.9. Statistical analysis

The statistical analysis of data was done by SPSS software using one-way ANOVA. Quantitative (cellular) data were depicted as means ± standard deviations (SD) of three experiments. The significance level was considered at the $P < 0.05$. All detected spectra were corrected for buffer and calycosin signals.

3. Results and discussion

3.1. Fluorescence quenching study

The fluorescence quenching of proteins can be evaluated by analyzing the intrinsic fluorescence intensity of the receptor before and after integration with ligands (Zargar et al., 2022, Zhao et al., 2022). Fluorescence spectroscopy experiment provides useful data regarding the molecular interaction in a vicinity of the aromatic amino acid residues (Xue et al., 2017). The interaction of calycosin with HSA and resultant fluorescence quenching was depicted in Fig. 1a. When increasing concentrations of calycosin solution were interacted with a fixed amount of HSA, a considerable fluorescence quenching of HSA was detected, which designated that calycosin can potentially interact with HSA. Also, from Fig. 1a, the emission λ_{max} of HSA shifted partially from 336 nm to 334 nm after the titration of calycosin, indicating the occurrence of a slight blue shift of emission λ_{max} (Naik et al., 2022). Generally, this data indicates that the aromatic residues of HSA were replaced in a more hydrophobic microenvironment after interaction with calycosin (Naik et al., 2022). The quantitative analysis of the interaction of calycosin with HSA was done based on the fluorescence quenching at 336 nm at different temperatures as displayed in Fig. 1b. It was observed that with the elevation of the concentration of calycosin, the fluorescence quenching of protein gradually increased, and with the further titration of calycosin, the fluorescence quenching decreased in a slower rate compared to lower concentrations of calycosin, which suggests saturation of the HSA binding site(s). Based on Eq. (1), the K_{SV} values were determined to be 0.07×10^6 M^{-1}, 0.05×10^6 M^{-1} and 0.02×10^6 M^{-1} at 298 K, 308 K and 318 K, respectively (Table 1). The reduction in K_{SV} values with increasing temperature indicated the occurrence of static quenching mechanism after interaction of calycosin and HSA (Banu et al., 2022). Also, k_q values were in the order of 10^{14} M^{-1} s^{-1} (Table 1), much greater than the dynamic quenching constant value (10^8 M^{-1} s^{-1}) (Niu et al., 2023), further supporting the fact that the fluorescence quenching of HSA after addition of calycosin is based on a static mechanism.

3.2. Calculation of binding parameters

The intrinsic fluorescence of HSA was determined at 336 nm after excitation at 280 nm. Utilizing the Eq. (2), binding parameters (K_b and n values) were determined for the complexation of calycosin with HSA at different temperatures.

Fig. 1c exhibits the modified Stern–Volmer plots for the calycosin–HSA system at different temperatures. The K_b and n values calculated from Eq. (2) based on this figure are sum-

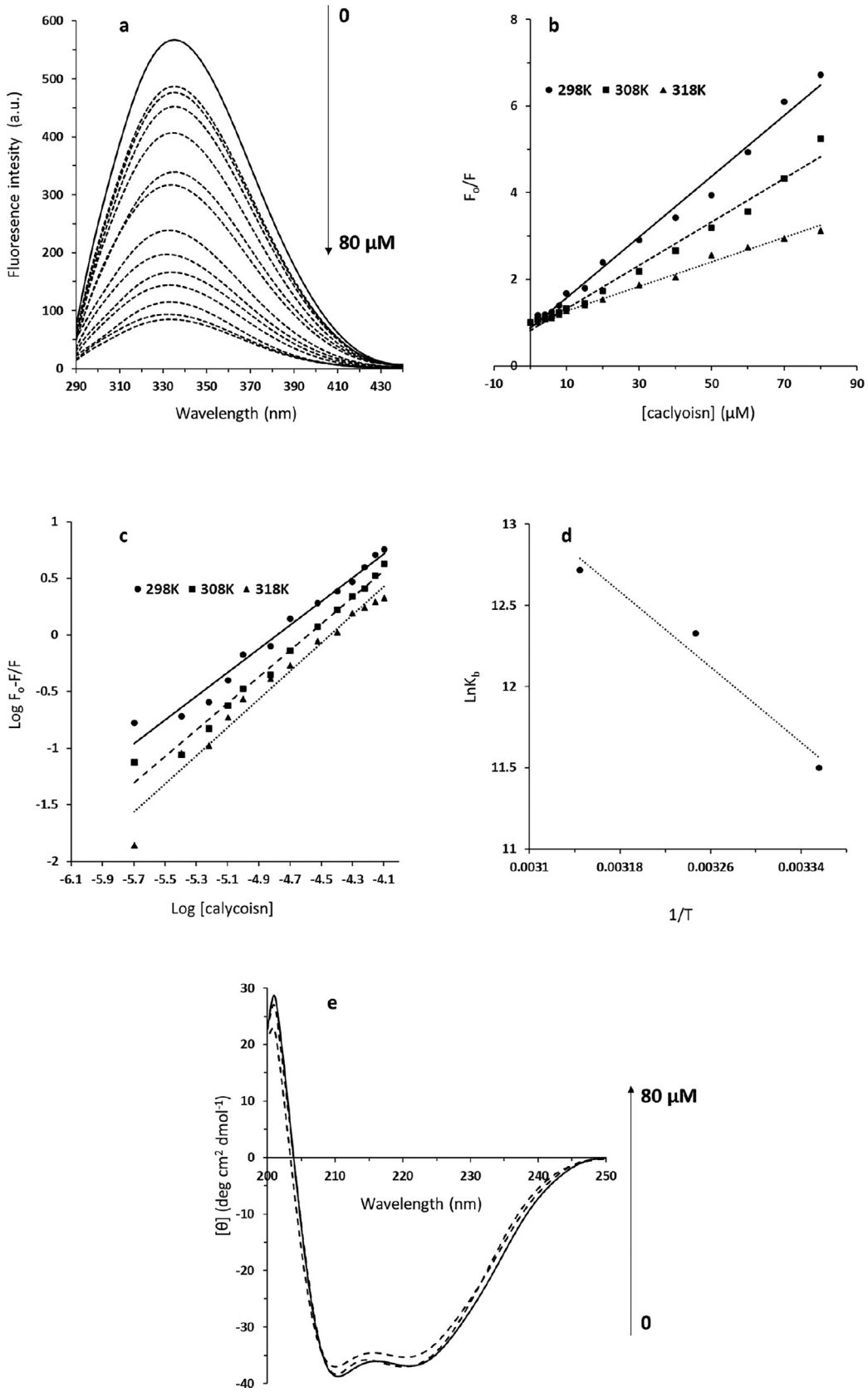

Fig. 1 (a) The fluorescence spectra of HSA (2 μM) interacted with different concentrations of calycosin (λex = 280 nm) at 298 K. The concentration of calycosin was 0–80 μM from the top to the bottom with the concentration intervals of 0, 2, 4, 6, 8, 10, 15, 20, 30, 40, 50, 60, 70, 80 μM. (b) Stern-Volmer plot for the interaction of calycosin and HSA. (c) Modified Stern-Volmer plot for the interaction of calycosin and HSA. (d) van't hoff plot for the interaction of calycosin and HSA. (e) Circular dichroism study for the interaction of calycosin and HSA.

Table 1 Interaction parameters of calycosin-HSA complex at 298 K, 308 K, and 318 K.

T (K)	K_{sv} (10^6 M^{-1})	k_q (10^{14} M^{-1} s^{-1})	K_b (10^5 M^{-1})	n	$\Delta H°$ (kJ mol^{-1})	$\Delta S°$ (J mol^{-1} K^{-1})	$\Delta G°$ (kJ mol^{-1})
298	0.07	0.07	1	1.04	48.10	257.38	−38.59
308	0.05	0.05	2.32	1.17	48.10	257.38	−31.68
318	0.02	0.02	3.39	1.24	48.10	257.38	−32.96

marized in Table 1. It can be inferred that the interaction between calycosin and HSA is very strong and the binding affinity increased with elevating temperature (Fig. 1c, Table 1), concluding that calycosin–HSA system is thermodynamically more stable at higher temperature than lower ones (Khan et al., 2020). Also, it was demonstrated that HSA has almost more than one binding site for calycosin, and it also increased partially with increasing temperature. It may be suggested that the elevation of temperature gives rise to some partial conformational changes on the surface of HAS (Yeggoni et al., 2022), favoring the interaction of calycosin with HSA.

3.3. Determination of binding mode

For the purpose of determining the interaction between calycosin and HSA, the thermodynamic parameters were estimated from the Van't Hoff plots (Fig. 1d) based on Eq. (3). The temperatures used were 298, 308, and 318 K. The $\Delta H°$ and $\Delta S°$ values were calculated from the slope and intercept of the van't Hoff equation.

Fig. 1d depicts the van't Hoff plot of the calycosin-HSA system at different temperatures. Table 1 tabulates the $\Delta H°$ and $\Delta S°$ values determined for the binding site(s) and it was revealed that $\Delta H°$ and $\Delta S°$ values were around 48.10 kJ mol^{-1} and 257.38 J mol^{-1} K^{-1}, respectively. The calculated negative $\Delta G°$ value (-28.59 kJ mol^{-1}), calculated from Eq. (4), means that a spontaneous interaction occurs between calycosin and HSA (Zhang et al., 2023). For ligand–receptor interaction, positive entropy is substantially associated with hydrophobic interaction and partially with hydrogen bonding (Ali et al., 2022). Hence, we may conclude that the interaction of calycosin with HSA is mainly driven by hydrophobic contact, however the hydrogen bonding interaction cannot be ignored.

3.4. CD spectra

To gain some details about the secondary structure of the HSA, far-UV CD analysis was done for the calycosin–HSA system. In the Far-UV region, such ellipticity changes are derived from the polypeptide backbone electrons (Qureshi et al., 2022). The comparison of the Far-UV CD spectra of HSA with calycosin–HSA is exhibited in Fig. 1e at room temperature. The ellipticity changes of HSA displayed two negative minima around 209 and 221 nm, signifying a typical α-helix secondary structure (Du et al., 2023). The interaction between calycosin with two concentrations of 10 and 80 μM and HSA led to only a partial reduction in ellipticity changes of two negative minima without any apparent blue or red shift of the peaks, specifying the induction of a slight reduction in the helix structure amount of the HSA (Tian-Zhu et al., 2022). Based on CD software, it was realized that the α-helix content of HSA was reduced from 58.21% to 54.69%. From CD and fluorescence spectra, we can infer that the interaction of calycosin with HSA occurs mainly through involvement of hydrophobic amino acid residues which then triggers a slight unfolding of the HSA polypeptide.

3.5. Molecular docking (MD) analysis

The MD analysis can provide us with useful details regarding the binding site after interaction between ligands and receptors (Rahman et al., 2022). This is crucial to understand if ligands can be used for the development of therapeutic platforms. The binding details will also give us some insights to realize if the ligand under study will interfere with the interactions of the receptor with other ligands and drugs. Fig. 2a exhibits the structure of calycosin, while Fig. 2b displays the HSA structure with the box coordinates. The binding energy was calculated to be in the range of –7.7 to −8.4 kcal mol^{-1}, revealing a strong affinity between HSA and calycosin compound (Fig. 2c). Then, the main amino acid residues placed in the interaction site of HSA with calycosin are displayed in Fig. 2d. It was presented that C7, C9, C15, C2, C10, C13, and C7 from ligand atoms interact with E119 (A) CB, V120 (A) CB, K174 (A) CD, A175 (A) CB, E119 (B) CG, K174 (B) CB, and A175 (B) CB, respectively, through involvement of hydrophobic forces. Also, it was illustrated that O4, O1, O2, and O3 from ligand atoms interact with D173 (B) OD1, V120 (B) N, D121 (A) N, and K174 (B) N, respectively through contribution of hydrogen bond. These data are in good agreement with fluorescence quenching data, which indicated that hydrophobic forces are the main involved interaction in the formation of calycosin-HSA system.

3.6. Cytotoxicity assay

The effect of calycosin on breast cancer cells, MDA-MB 231, found that this bioactive material induced anticancer effects at high concentrations (IC_{50}: 200 μM), suggesting that at higher concentrations, calycosin probably interfere with several cell signaling pathways, leading to an inhibition of cell proliferation (Fig. 3a). The effect of calycosin on normal human breast epithelial cells, MCF-10A, denoted a negligible cytotoxic effect. In the concrete, the MTT results displayed that calycosin did not significantly mitigate the viability of human normal breast cells, MCF-10A, even at 200 μM concentration at which this bioactive material is able to inhibit the proliferation of cancer cells up to 50%. Cytotoxicity of

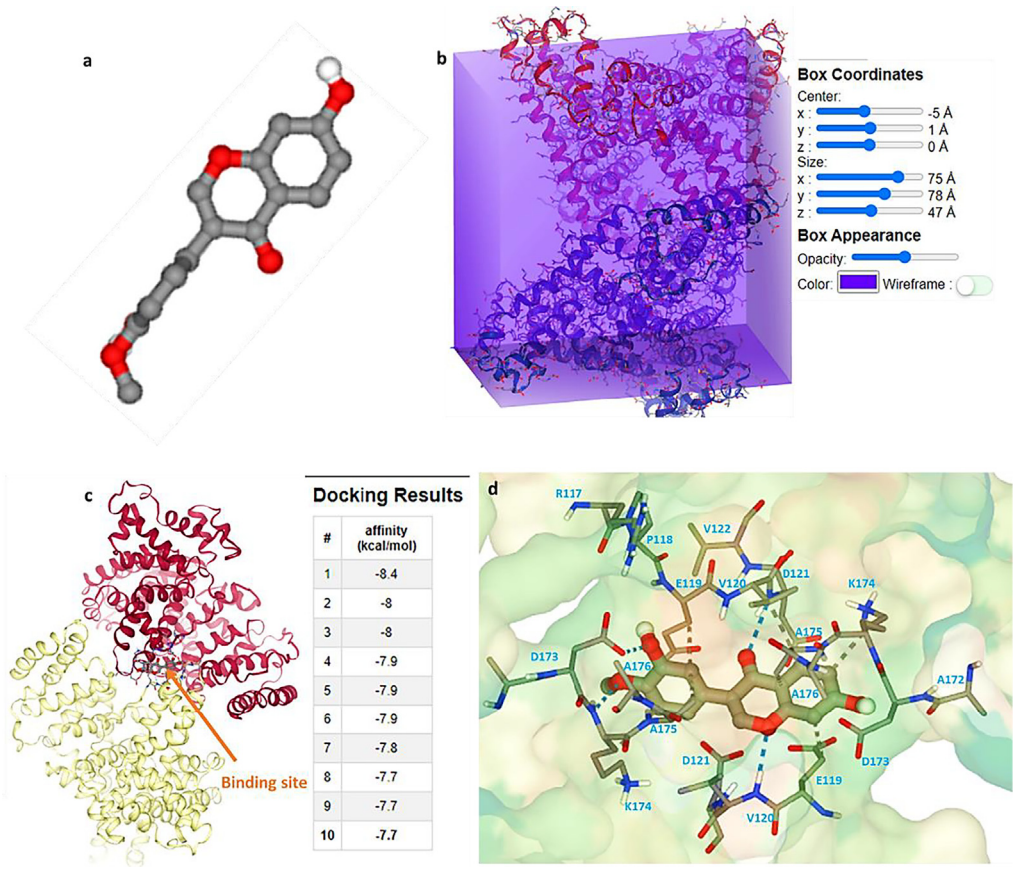

Fig. 2 (a) The structure of calycosin, (b) box coordinates for interaction of HSA and calycosin, (c) binding pocket of HSA after interaction with calycosin, (d) amino acid residues presented in the binding pocket.

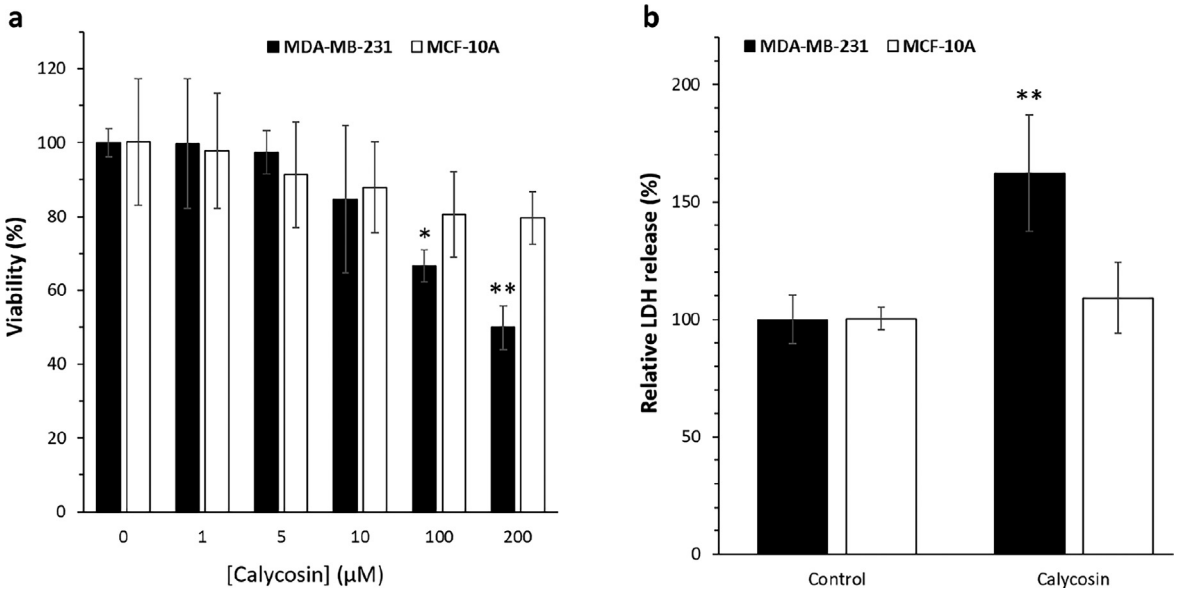

Fig. 3 Cell viability and membrane leakage assay by calycosin incubation. Breast cancer MDA-MB 231 cells were incubated with calycosin with 200 μM concentrations for 48 h. (a) The cell viability assay determined by MTT assay, (b) the cell membrane leakage determined by LDH assay. Data were expressed as mean ± SD, in three assays. Compared to the control group, *P < 0.05 and **P < 0.01.

calycosin (200 μM) against breast cancer MDA-MB 231 cells was 2.4 times more severe than its cytotoxicity against MCF-10A normal breast cells after 48 h incubation of cells. Actually, the different ways that calycosin interacts with normal and cancer cells, particularly the way that it leads to membrane leakage, may accentuate the differences between the more cytotoxic effects of calycosin on cancer cells versus normal cells. To further support this probable effect, we perform LDH assay after incubation of cells with 200 μM calycosin for 48 h. As depicted in Fig. 3b, the relative LDH release (%) increased to 1.62% and 1.9% after incubation of breast cancer MDA-MB 231 cells and MCF-10A normal breast cells, respectively, with calycosin. It was then realized that calycosin can selectively trigger membrane leakage in cancer cells, which may be assisted with different receptors and membrane compositions between cancer and normal cells. Additionally, it was evinced that formononetin, an O-methylated isoflavone like calycosin, did not significantly produce a cytotoxic effect against breast cancer MDA-MB 231 cells up to 80 M after 24 h (Zhou et al., 2014). However, the IC_{50} values of biochanin A in mitigating the proliferation of MDA-MB-231 cells was 63.76 μM (Ren et al., 2018), indicating that this small molecule can be combined with calycosin in the future studies to may intensify the anticancer effects of calycosin.

3.7. Impacts of calycosin-triggered MDA-MB 231 cell apoptosis

Investigation was performed to assess the apoptosis induction by calycosin in MDA-MB 231 cells by using a real-time PCR analysis. The Bcl-2 family is known to act as important regulators of the intrinsic pathway contributed in apoptosis induction. To explore whether calycosin could control the expression of the Bcl-2 family such as Bax and Bcl-2 mRNA, real-time PCR was performed to quantify the expression levels of these genes. Fig. 4 exhibited that calycosin at the concentration of 200 μM could elevate Bax mRNA level (Fig. 4a) while reducing Bcl-2 mRNA level (Fig. 4b) in MDA-MB 231 cells. These data declared that the stimulation of calycosin on apoptosis might be related with Bax and Bcl-2 deregulation.

Caspases, known as a family of cysteine acid proteases, are responsible for mediating apoptosis induction. Caspase overexpression derived from cytochrome *c* release can result in triggering of apoptosis. In this paper, it was expressed that the incubation of calycosin elevated the expressions of caspase-3 mRNA (Fig. 4c) and activity of caspase-3 (Fig. 4d), as the final target of apoptosis induction. It suggested that calycosin triggered apoptosis of breast cancer MDA-MB 231 cells via regulation of Bax, Bcl-2, caspase-3 signaling pathway.

Apoptosis is firmly linked with cancer therapy and previous reports have shown that apoptosis promoters can be utilized as potential candidates for cancer therapy (Bold et al., 1997). In advanced types of tumors, interfering in apoptosis-mediated signaling cascades has been recommended as one of the potential strategies for inhibiting the cancer cell proliferation (Carneiro and El-Deiry, 2020). Calycosin has been manifested to mitigate the proliferation of several types of cancer cells and to trigger cell death by an apoptotic mechanism (Wang et al., 2021, Zhang et al., 2021, Wei et al., 2023). It has been displayed that calycosin can stimulate apoptosis in cervical cancer via modulation of tumor suppressor miR-375 (Zhang et al., 2020). Also, it was reported that inhibition of Rab27B-mediated signaling cascade by calycosin can lead to inhibition of migration and metastasis of estrogen-negative breast cancer cells (Wu et al., 2019). Nevertheless, it is not well-evidenced about the role of calycosin interaction between apoptosis and breast tumor cells. During cytotoxicity, Bax, Bcl-2, and caspase-3 are reliable apoptosis markers. Thus, to reveal the role of calycosin in apoptosis induction, expression levels of these markers were analyzed using real-time PCR. The results exhibited that calycosin can upregulate the expression of levels of apoptotic genes, Bax and caspase-3 mRNA, and concomitantly reduced Bcl-2 mRNA expression as an antiapoptotic gene. These outcomes disclosed that the cytotoxic impacts of calycosin in breast cancer MDA-MB 231 cells may at least in part be derived from the induction of apoptosis.

3.8. Calycosin triggers apoptosis through the AKT/mTOR signaling pathway

Thus far our data implied that calycosin could significantly trigger apoptosis in breast cancer MDA-MB 231 cells. Given the crucial role of PI3K/Akt/mTOR signaling pathway in regulating cell proliferation in several types of tumor cells, including breast cancer cells (Miricescu et al., 2020), we analyzed whether calycosin triggered apoptosis through the inhibition of PI3K/Akt/mTOR signaling pathway.

To explore the involvement of this signaling pathway, two important molecules, Akt and mTOR at the mRNA level, were assessed. The expression of Akt as well as mTOR mRNA was determined in breast cancer MDA-MB 231 cells by quantitative real time-PCR (Fig. 5a and b). As expected, in comparison with the control group, 200 μM of calycosin substantially mitigated the expression level of mTOR (0.60 ± 0.09) (**$P < 0.01$), as expressed in Fig. 5a. As depicted in Fig. 5b, the expression of Akt mRNA in the calycosin-treated group (0.75 ± 0.14) (*$P < 0.05$), was remarkably lower than that determined in control samples (1.04 ± 0.09) ($P < 0.01$). In order to further support and determine the role of mTOR and Akt in the calycosin-regulation PI3K/Akt/mTOR signaling pathway in breast cancer MDA-MB 231 cells, the influence of rapamycin and LY294002 as inhibitors of mTOR and PI3K/Akt, respectively was investigated (Chen et al., 2014b). It was shown that similar to the impact of calycosin, there was a more remarkable inhibitory impact on mTOR and Akt mRNA levels when it co-incubated with the inhibitory molecules compared with calycosin-treated samples (Fig. 5a and b). Collectively, these data ascertained that calycosin-triggered apoptosis was due, at least in part, to mitigation of the AKT/mTOR signaling pathway. In other words, our data uncovered that calycosin may exert cytotoxic impact on breast cancer MDA-MB 231 cells through inhibiting the PI3K/Akt/mTOR signaling pathway to induce apoptosis, declaring that PI3K/Akt/mTOR signaling pathway is a crucial pathway contributed in the role of calycosin -mediated breast cancer cell death, and might be also one of the main targets of calycosin.

Apoptosis is modulated by several upstream signaling pathways. The AKT/mTOR signaling pathway is documented as an important mechanism that controls a number of cellular pathways in cancer cells, such as cell proliferation, growth, and migration (Khan et al., 2019). mTOR is known to be

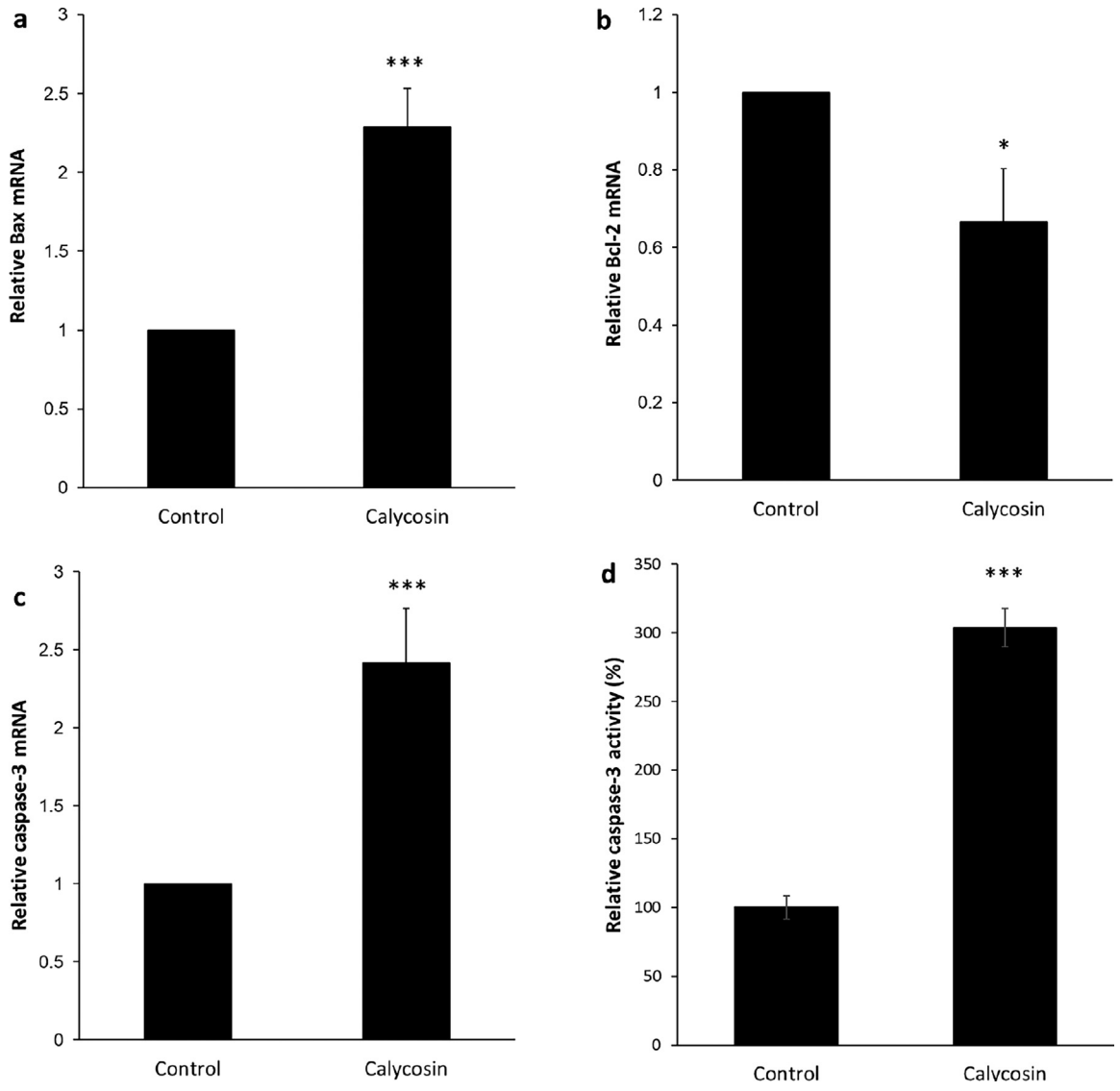

Fig. 4 Apoptosis induction by calycosin incubation. Breast cancer MDA-MB 231 cells were incubated with calycosin with 200 μM concentrations for 48 h. (a) The expression of Bax mRNA as determined by quantitative real-time PCR, (b) the expression of Bcl-2 mRNA as determined by quantitative real-time PCR, (c) the expression of caspase-3 mRNA as determined by quantitative real-time PCR, (d) caspase-3 activity assay. Data were expressed as mean ± SD, in three assays. Compared to the control group, *P < 0.05 and ***P < 0.001.

phosphorylated by AKT and p-mTOR negatively modulates apoptosis (Peng et al., 2022). It has been indicated that bioactive materials can target AKT/mTOR signaling cascade in cancer cells (Tewari et al., 2022). Blockade of the AKT/mTOR pathway was realized to trigger the induction of apoptosis to provide anticancer impacts (Liu et al., 2023, Sawasdee et al., 2023). Some other types of O-methylated isoflavones, including tectorigenin, formononetin, and glycitein have been expressed to induce anticancer effects through regulation of PI3K/AKT/mTOR pathway. For example, tectorigenin has been able to increase the sensitization of anticancer drug-resistant human ovarian cancer cells via regulation of the Akt as well as NF-κB signaling cascade (Yang et al., 2012). Moreover, formononetin was exhibited to inhibit proliferation and migration of MDA-MB-231 as well as 4T1 breast cancer cells by inhibiting PI3K/AKT signaling cascade (Zhou et al., 2014). Furthermore, it was reported that PI3K/AKT signaling cascade is one of the main mechanisms of glycitein in the inhibition of colon cancer cell proliferation (Xiang and Jin, 2023). The present report presented whether the AKT/mTOR signaling cascade might be involved in the apoptosis upregulation potency of calycosin. As a matter of fact, calycosin treatment remarkably mitigated the expression levels of AKT and mTOR mRNA in breast cancer MDA-MB 231 cells. Collectively, the data from this study demonstrated that the AKT/mTOR signaling cascade was involved in calycosin-induced apoptosis in breast cancer MDA-MB 231 cells.

4. Conclusion

In this paper, we explored the interaction of calycosin with HSA by spectroscopic studies as well as MD analysis. The experimental outcomes disseminated that calycosin can bind with HSA strongly with

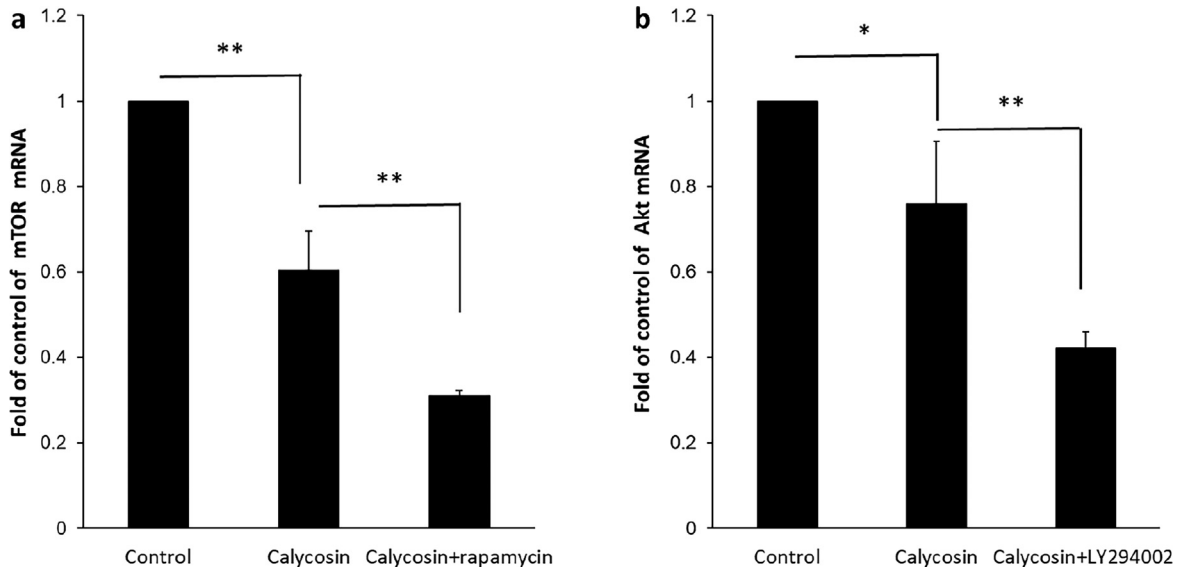

Fig. 5 Signal transduction study by calycosin incubation. Breast cancer MDA-MB 231 cells were incubated with calycosin with 200 μM concentrations for 48 h. Also, the treated cells were pre-treated with rapamycin (40 μM) or LY294002 (20 μM) for 4 h. Control cells did not receive any treatment. (a) The expression of mTOR mRNA, (b) the expression of Akt mRNA, analyzed by the quantitative real-time PCR assay. Data were expressed as mean ± SD, in three assays. Compared to the control group, *P < 0.05 and **P < 0.01.

the involvement of hydrophobic interaction, which induced a partial secondary structural change of HSA. MD analysis also verified that hydrophobic amino acids were the majority of residues that existed in the binding site of HSA with calycosin. Cellular and molecular studies determined that, in breast cancer MDA-MB 231 cells, calycosin (IC_{50}: 200 μM) could suppress cellular proliferation by inducing apoptosis, which are controlled by the AKT/mTOR signaling cascade.

Funding

This study was supported by National Natural Science Foundation of China (No. 82002818), Tianjin Medical University's "Clinical Talent Development 123 Climbing Plan"(NO.2022), and General Project of Scientific Research Program of Tianjin Municipal Education Commission (No. 2019KJ184).

Declaration of Competing Interest

The authors declare that they have no known competing financial interests or personal relationships that could have appeared to influence the work reported in this paper.

References

Ali, M.S., Rehman, M.T., Al-Lohedan, H.A., AlAjmi, M.F., 2022. Exploration of the binding between cuminol and bovine serum albumin through spectroscopic, molecular docking and molecular dynamics methods. J. Biomol. Struct. Dyn. 40 (22), 12404–12412.

Banu, A., Khan, R.H., Qashqoosh, M.T.A., Manea, Y.K., Furkan, M., Naqvi, S., 2022. Multispectroscopic and computational studies of interaction of bovine serum albumin, human serum albumin and bovine hemoglobin with bisacodyl. J. Mol. Struct. 1249, 131550.

Bold, R.J., Termuhlen, P.M., McConkey, D.J., 1997. Apoptosis, cancer and cancer therapy. Surg. Oncol. 6 (3), 133–142.

Carneiro, B.A., El-Deiry, W.S., 2020. Targeting apoptosis in cancer therapy. Nat. Rev. Clin. Oncol. 17 (7), 395–417.

Chen, J., Hou, R., Zhang, X., Ye, Y., Wang, Y., Tian, J., 2014a. Calycosin suppresses breast cancer cell growth via ERβ-dependent regulation of IGF-1R, p38 MAPK and PI3K/Akt pathways. PLoS One 9 (3), e91245.

Chen, L., Li, Z., Tang, Y., Cui, X., Luo, R., Guo, S., Zheng, Y., Huang, C., 2011. Isolation, identification and antiviral activities of metabolites of calycosin-7-O-β-d-glucopyranoside. J. Pharm. Biomed. Anal. 56 (2), 382–389.

Chen, J., Lin, C., Yong, W., Ye, Y., Huang, Z., 2015a. Calycosin and genistein induce apoptosis by inactivation of HOTAIR/p-Akt signaling pathway in human breast cancer MCF-7 cells. Cell. Physiol. Biochem. 35 (2), 722–728.

Chen, Z., Yang, L., Liu, Y., Tang, A., Li, X., Zhang, J., Yang, Z., 2014b. LY294002 and Rapamycin promote coxsackievirus-induced cytopathic effect and apoptosis via inhibition of PI3K/AKT/mTOR signaling pathway. Mol. Cell. Biochem. 385, 169–177.

Chen, J., Zhao, X., Li, X., Wu, Y., 2015b. Calycosin induces apoptosis by the regulation of ERβ/miR-17 signaling pathway in human colorectal cancer cells. Food Funct. 6 (9), 3091–3097.

Dong, L., Yin, L., Chen, R., Zhang, Y., Hua, S., Quan, H., Fu, X., 2018. Anti-inflammatory effect of Calycosin glycoside on lipopolysaccharide-induced inflammatory responses in RAW 264.7 cells. Gene 675, 94–101.

Du, X., Yao, J., Li, H., Bao, Y., Lan, J., Zhao, Z., Zong, W., 2023. Study on the interaction between sulfamerazine and human serum albumin on molecular level using spectral analysis. Colloids Surf. A Physicochem. Eng. Asp. 661, 130917.

Fattahian Kalhor, N., Saeidifar, M., Ramshini, H., Saboury, A.A., 2020. Interaction, cytotoxicity and sustained release assessment of a novel anti-tumor agent using bovine serum albumin nanocarrier. J. Biomol. Struct. Dyn. 38 (9), 2546–2558.

Gao, J., Liu, Z.J., Chen, T., Zhao, D., 2014. Pharmaceutical properties of calycosin, the major bioactive isoflavonoid in the dry root extract of Radix astragali. Pharm. Biol. 52 (9), 1217–1222.

He, Y., Wang, Y., Tang, L., Liu, H., Chen, W., Zheng, Z., Zou, G., 2008. Binding of puerarin to human serum albumin: a spectroscopic analysis and molecular docking. J. Fluoresc. 18 (2), 433–442.

Huang, D., Shen, P., Wang, C., Gao, J., Ye, C., Wu, F., 2022. Calycosin plays a protective role in diabetic kidney disease through the regulation of ferroptosis. Pharm. Biol. 60 (1), 990–996.
Khan, M.A., Jain, V.K., Rizwanullah, M., Ahmad, J., Jain, K., 2019. PI3K/AKT/mTOR pathway inhibitors in triple-negative breast cancer: a review on drug discovery and future challenges. Drug Discov. Today 24 (11), 2181–2191.
Khan, I.M., Shakya, S., Akhtar, R., Alam, K., Islam, M., Alam, N., 2020. Exploring interaction dynamics of designed organic cocrystal charge transfer complex of 2-hydroxypyridine and oxalic acid with human serum albumin: Single crystal, spectrophotometric, theoretical and antimicrobial studies. Bioorg. Chem. 100, 103872.
Kragh-Hansen, U., 1990. Structure and ligand binding properties of human serum albumin. Dan. Med. Bull. 37 (1), 57–84.
Liu, F., Mu, J., Xing, B., 2015. Recent advances on the development of pharmacotherapeutic agents on the basis of human serum albumin. Curr. Pharm. Des. 21 (14), 1866–1888.
Liu, F., Gao, S., Yang, Y., Zhao, X., Fan, Y., Ma, W., Yang, D., Yang, A., Yu, Y., 2018. Antitumor activity of curcumin by modulation of apoptosis and autophagy in human lung cancer A549 cells through inhibiting PI3K/Akt/mTOR pathway. Oncol. Rep. 39 (3), 1523–1531.
Liu, T., Gong, J., Lai, G., Yang, Y., Wu, X., Wu, X., 2023. Flavonoid extract Kushenol a exhibits anti-proliferative activity in breast cancer cells via suppression of PI3K/AKT/mTOR pathway. Cancer Med. 12 (2), 1643–1654.
Liu, X., Sun, X., Deng, X., Lv, X., Wang, J., 2020. Calycosin enhances the bactericidal efficacy of polymyxin B by inhibiting MCR-1 in vitro. J. Appl. Microbiol. 129 (3), 532–540.
Memmott, R.M., Dennis, P.A., 2009. Akt-dependent and-independent mechanisms of mTOR regulation in cancer. Cell. Signal. 21 (5), 656–664.
Miricescu, D., Totan, A., Stanescu-Spinu, I.-I., Badoiu, S.C., Stefani, C., Greabu, M., 2020. PI3K/AKT/mTOR signaling pathway in breast cancer: from molecular landscape to clinical aspects. Int. J. Mol. Sci. 22 (1), 173.
Naik, R., Pawar, S., Seetharamappa, J., 2022. Elucidating the binding mechanism of a cholesterol absorption inhibitor with a serum albumin: spectroscopic, zeta potential, voltammetric and computational studies. Chem. Pap. 76 (7), 4017–4031.
Niu, T., Zhu, X., Zhao, D., Li, H., Yan, P., Zhao, L., Zhang, W., Zhao, P., Mao, B., 2023. Unveiling interaction mechanisms between myricitrin and human serum albumin: Insights from multi-spectroscopic, molecular docking and molecular dynamic simulation analyses. Spectrochim. Acta A Mol. Biomol. Spectrosc. 285, 121871.
Peng, Y., Wang, Y., Zhou, C., Mei, W., Zeng, C., 2022. PI3K/Akt/mTOR pathway and its role in cancer therapeutics: are we making headway? Front. Oncol. 12, 819128.
Qu, N., Qu, J., Huang, N., Zhang, K., Ye, T., Shi, J., Chen, B., Kan, C., Zhang, J., Han, F., 2022. Calycosin induces autophagy and apoptosis via Sestrin2/AMPK/mTOR in human papillary thyroid cancer cells. Front. Pharmacol. 13.
Qureshi, M.A., Akbar, M., Amir, M., Javed, S., 2022. Molecular interactions of esculin with bovine serum albumin and recognition of binding sites with spectroscopy and molecular docking. J. Biomol. Struct. Dyn., 1–15
Rahman, N., Khalil, N., Khan, S., Almutairi, M.H., Almutairi, B.O., Alam, M., 2022. Multispectroscopic and molecular docking studies on the interaction of diltiazem hydrochloride with bovine serum albumin and its application to the quantitative determination of diltiazem hydrochloride. J. King Saud Univ.-Sci. 34, (7) 102267.
Ren, G., Shi, Z., Teng, C., Yao, Y., 2018. Antiproliferative activity of combined Biochanin A and Ginsenoside Rh2 on MDA-MB-231 and MCF-7 human breast cancer cells. Molecules 23 (11), 2908.
Roy, A.S., Tripathy, D.R., Chatterjee, A., Dasgupta, S., 2013. The influence of common metal ions on the interactions of the isoflavone genistein with bovine serum albumin. Spectrochim. Acta A Mol. Biomol. Spectrosc. 102, 393–402.
Sawasdee, N., Jantakee, K., Wathikthinnakon, M., Panwong, S., Pekkoh, J., Duangjan, K., Yenchitsomanus, P.-T., Panya, A., 2023. Microalga Chlorella sp. extract induced apoptotic cell death of cholangiocarcinoma via AKT/mTOR signaling pathway. Biomed. Pharmacother. 160, 114306.
Schmittgen, T.D., Livak, K.J., 2008. Analyzing real-time PCR data by the comparative CT method. Nat. Protoc. 3 (6), 1101–1108.
Song, J., Yang, J., Yang, J., Sun, G., Song, G., Li, J., Zhao, S., 2023. Regulation of Wnt/GSK3β/β-catenin signaling pathway regulates calycosin-mediated anticancer effects in glioblastoma multiforme cells. Arab. J. Chem. 104567
Takahashi, I., Ohnuma, T., Kavy, S., Bhardwaj, S., Holland, J.F., 1980. Interaction of human serum albumin with anticancer agents in vitro. Br. J. Cancer 41 (4), 602–608.
Tewari, D., Patni, P., Bishayee, A., Sah, A.N., Bishayee, A., 2022. Natural products targeting the PI3K-Akt-mTOR signaling pathway in cancer: A novel therapeutic strategy. Seminars in cancer biology. Elsevier.
Tian, J., Wang, Y., Zhang, X., Ren, Q., Li, R., Huang, Y., Lu, H., Chen, J., 2017. Calycosin inhibits the in vitro and in vivo growth of breast cancer cells through WDR7-7-GPR30 Signaling. J. Exp. Clin. Cancer Res. 36 (1), 1–13.
Tian-Zhu, G., Ning, L.I., Ya, G.A.O., Ya-Jun, G.A.O., Ming, Y., Qiong, L.I., Li-Xia, X., 2022. Mechanism evaluation of the interactions between bisphenol AP and bovine serum albumin based on multi-spectroscopy, wavefunction analysis, and molecular docking. Chin. J. Anal. Chem. 50, (6) 100099.
Wang, X.-Z., Zhang, X.-Y., Mu, Y., Xia, L., Zhang, Y.-N., 2021. Anti-tumor effect and mechanisms of calycosin: A review. Chin. J. Exp. Tradit. Med. Formulae, 210–217.
Wang, J., Zhang, J., Zhao, Y., 2023. Calycosin Alleviates oxidative stress and pyroptosis induced by high glucose in human retinal capillary endothelial cells induced by high glucose. Curr. Top. Nutraceut. Res. 21 (1).
Wei, X., Zeng, Y., Meng, F., Wang, T., Wang, H., Yuan, Y., Li, D., Zhao, Y., 2023. Calycosin-7-glucoside promotes mitochondria-mediated apoptosis in hepatocellular carcinoma by targeting thioredoxin 1 to regulate oxidative stress. Chem. Biol. Interact. 110411
Wu, G., Niu, M., Qin, J., Wang, Y., Tian, J., 2019. Inactivation of Rab27B-dependent signaling pathway by calycosin inhibits migration and invasion of ER-negative breast cancer cells. Gene 709, 48–55.
Xiang, T., Jin, W., 2023. Mechanism of glycitein in the treatment of colon cancer based on network pharmacology and molecular docking. Lifestyle Genomics 16, 1–10.
Xue, Z., Cheng, A., Li, Y., Yu, W., Kou, X., 2017. Investigating interaction between Biochanin A and human serum albumin by multi-spectroscopic and molecular simulation methods. Trans. Tianjin Univ. 23, 325–333.
Yang, Y.-I., Lee, K.-T., Park, H.-J., Kim, T.J., Choi, Y.S., Shih, I.-M., Choi, J.-H., 2012. Tectorigenin sensitizes paclitaxel-resistant human ovarian cancer cells through downregulation of the Akt and NFκB pathway. Carcinogenesis 33 (12), 2488–2498.
Yeggoni, D.P., Dubey, S., Mohammad, Y.Z., Rachamallu, A., Subramanyam, R., 2022. Elucidation of binding mechanism of stigmasterol with human serum albumin: a biophysical and molecular dynamics simulation approach. J. Biomol. Struct. Dyn. 40 (22), 12135–12147.
Zargar, S., Wani, T.A., Alsaif, N.A., Khayyat, A.I.A., 2022. A comprehensive investigation of interactions between antipsychotic drug quetiapine and human serum albumin using multi-spectroscopic, biochemical, and molecular modeling approaches. Molecules 27 (8), 2589.
Zhang, D., Sun, G., Peng, L., Tian, J., Zhang, H., 2020. Calycosin inhibits viability, induces apoptosis, and suppresses invasion of

cervical cancer cells by upregulating tumor suppressor miR-375. Arch. Biochem. Biophys. 691, 108478.
Zhang, H., Wang, S., Fan, W., Peng, P., Cheng, J., 2023. Albumin-binding properties of an aromatic N-acylhydrazone. J. Mol. Liq. 372, 121180.
Zhang, Y., Zhang, J.-Q., Zhang, T., Xue, H., Zuo, W.-B., Li, Y.-N., Zhao, Y., Sun, G., Fu, Z.-R., Zhang, Q., 2021. Calycosin induces gastric cancer cell apoptosis via the ROS-mediated MAPK/STAT3/NF-κB pathway. OncoTargets Therapy 14, 2505.
Zhao, J., Ren, F., 2009. Influence of hydroxylation and glycosylation in ring A of soybean isoflavones on interaction with BSA. Spectrochim. Acta A Mol. Biomol. Spectrosc. 72 (3), 682–685.
Zhao, J., Huang, L., Li, R., Zhang, Z., Chen, J., Tang, H., 2022. Multispectroscopic and computational evaluation of the binding of flavonoids with bovine serum albumin in the presence of Cu^{2+}. Food Chem. 385, 132656.
Zhou, R., Xu, L., Ye, M., Liao, M., Du, H., Chen, H., 2014. Formononetin inhibits migration and invasion of MDA-MB-231 and 4T1 breast cancer cells by suppressing MMP-2 and MMP-9 through PI3K/AKT signaling pathways. Horm. Metab. Res. 46 (11), 753–760.